Enhancement Performance of High Electron Mobility Transistor (HEMT) Based on Dimensions Downscaling

Firas Natheer Abdul-kadir[1, *], Nawfal Y. Jamil[2], Laith M. Al Taan[3], and Waheb A. Jabbar[4]

[1] Department of Electrical Engineering, College of Engineering, University of Mosul, Mosul, Iraq;
Email: firas_nadheer@uomosul.edu.iq*

[2] Department of Radiation Techniques, Alnoor University College, Mosul, Iraq; Email: nawfal@alnoor.edu.iq (N.Y.J.)

[3] Department of Physics, College of Science, University of Mosul Mosul, Iraq; Email: laithaltaan@uomosul.edu.iq
(L.M.A.T.)

[4] School of Engineering and the Built Environment, Birmingham City University, Birmingham B4 7XG, UK;
Email: waheb@ieee.org (W.A.J.)

Abstract—**This paper aims to enhance the performance of the High Electron Mobility Transistor (HEMT) according to downscaling dimensions based on the electrical properties and semiconductor materials (GaN, Si₃N₄, ALGaN and Si). This is to solve difficulties with reducing dimensions and ensuring HEMT has the highest performance possible. This goal was met when the physical scaling restrictions of channel diameters for different HEMTs were concurrently shrunk without compromising their performance. A simulation study was done using four variable factors (length, width, of the channel and length, width of the source and drain). Three electrical characteristics were used to assess the impact of altering dimensions on the performance of each kind of HEMT: threshold voltage V_t, ON-state/OFF-state current (I_{ON}/I_{OFF}) ratio, and transconductance g_m. To conduct experimental simulations under the specified situation, the well-known Silvaco TCAD simulation tool was used. The acquired simulation results revealed that the optimum performance for the downscaling device was achieved at the channel length of 1.6µm, the channel width of 0.3 µm, the length of source and drain is 0.4 µm and finally the width of source and drain is 0.05 µm.**

Index Terms—**GaN, High Electron Mobility Transistor (HEMT), channel length, downscaling, current gain**

I. INTRODUCTION

Since the early of 1990's, Field Effect Transistor (FET) has played a backbone of semiconductor devices. It represents the fundamental component of the system that uses modern technology in microelectronics designs [1]. The manufacturing progress of this transistor depends on the enhancement performance of FET [2]. The qualitative leap in performance of FET happened when new materials have been used in the structure of the transistor [3].

These materials including GaAs, GaP, GaN, Si₃N₄, ALGaN, GaSb, InAs, InSb, etc. have attracted significant attention from designers [4]. Also, have a considerable impact on the basic features of the device and is characterized by high mobility, high thermal conductivity, and high electrical breakdown [5, 6]. In the last years, a promising device that uses high mobility for charges (electrons) is the High Electron Mobility Transistor HEMT. This device (HEMT) is one of the most significant components that has played a major role and great influence in the design and development of microelectronics devices [7−9].

GaN-HEMT on a substrate of silicon has sparked a lot of attention because of their low cost and ability to scaling of Silicon. At the same time, GaN-HEMT on Silicon is surpass GaN-HEMT on a substrate of silicon carbide (SiC) according to enhancement Performance for the device [10−11]. The most important features of the HEMT based on GaN are the high frequency, high-temperature capability, and electric breakdown field is high and it has proven to be effective in high-power systems [12−14]. One new application of HEMT based on GaN is light emitting energy for Visual Light Communication (VLC), satellites, radar and sensor with high sensitivity [15].

The RF achievement of any transistor design is determined by the cutoff frequency "f_T" and the device's maximum frequency "f_{max}". In comparison to the fastest silicon CMOS transistor, GaN-based on HEMT is developing as applicable technology for high-fast and large-power applications [16, 17]. So GaN based on HEMT is outstanding to CMOS based on silicon transistor due to the wealth of material properties of gallium nitride such as big band gap (3.4 eV), large saturation velocity (2.5×10^5 m/s), large electron mobility (1600 cm²/V-s) and higher breakdown electric field (330 MV/m) [18−20]. GaN is a significant driver in optoelectronics and microwave circuits, and its expansion in the semiconductor industry is not confined to large-power electronics and radio-frequency devices [21]. Finally, GaN belongs to III and V group materials that offer spontaneous and piezoelectric polarization because of inherent non-centro symmetrical [22].

This paper is focused on simulation to enhance the performance of the High Electron Mobility Transistor (HEMT) based on dimensions downscaling for the device

not to solve the specified problem. The development of integrated circuits (ICs) has resulted from the scaling down of HEMT transistors from large to small dimensions [23]. The downscaling was done on the dimension of the device such as channel length (L_g), channel width (W_{ch}) and length of the source and drain (LSD) to investigate the performance of GaN HEMT in terms of threshold voltage, current drain ON-state, current drain OFF-state and transconductance ($g_m=\partial I_d/\partial V_g$). The saturation drain current in term of width to the length ratio of gate channel is given as: $I_d= \frac{1}{2}(\mu_n C_{ox})(W/L)(V_{gs}-V_{th})^2(1+\lambda\ V_{DS})$.

II. LITERATURE REVIEW

HEMTs are heterojunctions created by semiconductors with different band gaps, the conduction and valence bands must bend everywhere the material to make a continuous level when a heterojunction is formed [24−26]. The vast band gaps of material have doped with donor atoms have outrageous electrons through conduction band, while narrow band gaps of material (undoped) have lower energy in states of conduction band [27, 28].

Therefore, the diffusion process of electrons will happen between two different adjacent materials, wherein the electrons will move from wide band gap of one material to narrow band gap of another material. Thus and because of movement of these electrons, variation in potential will occur and induce an electrical field between two materials [29−32]. The influence of an electric field will make the electrons drift back to conduction state of wide band gap material.

The process of drift and diffusion of electrons is continuous until one balances the other, and so a P-N junction is forming at an equilibrium state [33, 34]. Finally, the majority of carriers of undoped narrow band gap material will excess and causes the high speed of switching. A fascinating point of the undoped semiconductor material is a narrow band gap has no donor atoms to generate scattering, thus ensuring excellent mobility [35, 36].

Another fascinating feature of HEMT is the discontinuous state between the valence and conduction bands which can be designed to control the kind of carriers that enter and exit the device [37]. The HEMT have a high current result of a process of diffusion electrons that will be accumulating these carriers through the confines of two area in narrow band gap material, these accumulated electrons are referred to as Two-Dimensional Electron Gas (2DEG) as in Fig. 1 [38, 40].
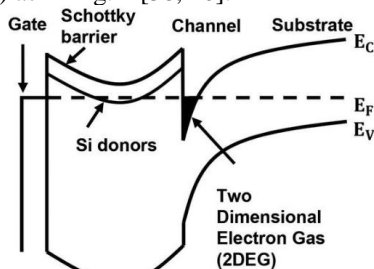
Fig. 1. Band diagram of a typical HEMT.

III. DEVICE STRUCTURE

GaN-based on HEMTs are made up of two materials with distinct band gaps, such as GaN and ternary alloy such as AlGaN. These materials (GaN and AlGaN) are highly advanced materials according to their structure of it. Fig. 1 shows schematic cross-sections of the HEMT that consist of a gate, source and drain made of conductor. The material under the gate is AlGaN, substrate material (under AlGaN) is GaN and insulator material on either side of the gate is Si_3N_4 [41, 42].

The basis on which the dimension of the device were taken into account is the result of several experimental attempts on the program (Silvaco) and the selection of the best results that obtained from it. So the channel length (L_g) of the gate is taken at several values (1.6 µm, 1.8 µm, 2 µm, 2.2 µm and 2.4 µm) and the channel width (W_{ch}) of the gate is taken at several values (0.3 µm, 0.4 µm and 0.5 µm). The length of the source and drain (Lds) are taken at (0.4 µm, 0.5 µm and 0.6 µm), and the width of the source and drain (W_{ds}) is (0.05µm and 0.1 µm). The work function of the gate (ϕ) is 5 eV and for the source and drain is 3.93 eV. The applied voltage at the drain terminal is 1 V, and the gate voltages are taken at (−3 V, −2 V, −1 V, 0 V). Silvaco TCAD was used to construct and simulate the device to investigate the influence of important parameters on the device, such as electrical characterization V_t, I_{ON}, I_{OFF}, I_{ON}/I_{OFF} and g_m. [43, 44].
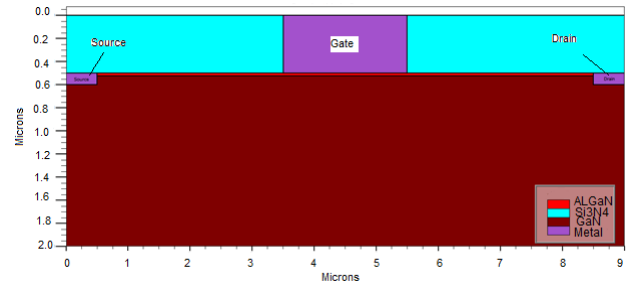
Fig. 2. Generalized structure of the HEMT.

IV. RESULTS AND DISCUSSIONS

In this section, we introduce the simulation results obtained from the Silvaco simulation (one dimension) to display the electrical characteristics for HEMT based on GaN. The simulation output curves of the device are taken under different variables and parameters are considered with parameters. The length of the channel (L_g) has been scaled (2.4 µm, 2.2 µm, 2.0 µm, 1.8 µm and 1.6 µm), whereas the width of the channel (W_{ch}) has been scaled (0.5 µm, 0.4 µm and 0.3 µm). The length of the source and drain (L_{ds}) has been scaled (0.6 µm, 0.5 µm and 0.4 µm). Finally, the width of the material GaN has been scaled (1.5 µm, 1.6 µm, 1.7 µm, 1.8 µm, 1.9 µm and 2 µm).

A. Downscaling Channel Length

Fig. 3 shows the transfer characteristics of drain current (I_d) with gate voltage (V_g) at different values of (L_g). We noticed that when the channel length is decreased the drain current is increased according to the

Equation $I_d=\frac{1}{2}(\mu_oC_{ox})(W_{ch}/L_g)(V_g-V_{th})^2$. Wherein the drain current is 34.40 mA at a channel length is 2.4 µm and the drain current is 34.56 mA at a channel length is 1.6 µm. Also, the threshold voltage (V_t) is reversely changed with channel length. Where the $V_t = -10.29$ V at $L_g = 2.4$ µm and $V_t = -13.56$ V at $L_g = 1.6$ µm. The figure demonstrates the device's effectiveness by showing that the I_d current will increase when the L_g decreases. That implies that the proportional between (I_d and L_g) is reversed. The reason for the improvement in drain current (I_{ON}) in the proposed device is the high electron mobility (μ) obtained due to the use of the InAs channel, along with the reduction in source/drain parasitic resistance due to the use of a heavily multilayer cap. Also, the HEMT gate may not show a finite resistance in the saturation region.

Fig. 4 shows the transconductance (g_m) against gate voltage (V_g) at different values of (L_g). We noticed that when the channel length decreases the transconductance is increased. Wherein the g_m is 27.87 m/s at a channel length is 2.4 µm and the g_m is 29.91 m/s at a channel length is 1.6 µm. Also, the figure confirms the device's

performance by validation relationship between (g_m and L_g), wherein, g_m will increase when the L_g decreases, here for high gain, the transconductance must be high.

B. Downscaling Channel Width

Fig. 5 presents transfer characteristics of drain current (I_d) with gate voltage (V_g) at different values of (W_{ch}). We noticed that when the channel width is decreased the drain current (I_{ON}) does not change (stable). The drain current is equal to 34.48 mA at channel width (0.5 µm, 0.4 µm and 0.3 µm). While threshold voltage (V_t) is directly proportional and changed with channel width, where V_t is equal to -12.09 V at $W_{ch} = 0.5$ µm and V_t is equal to -11.69 V at $W_{ch} = 0.3$ µm.

According to the drain current formula one can say, the resistance of the channel is inversely proportional to its width-to-length ratio; reducing the length leads to decreased resistance and hence higher current flow. Thus, channel-length modulation means that the saturation-region drain current will increase slightly as the drain-to-source voltage increases.
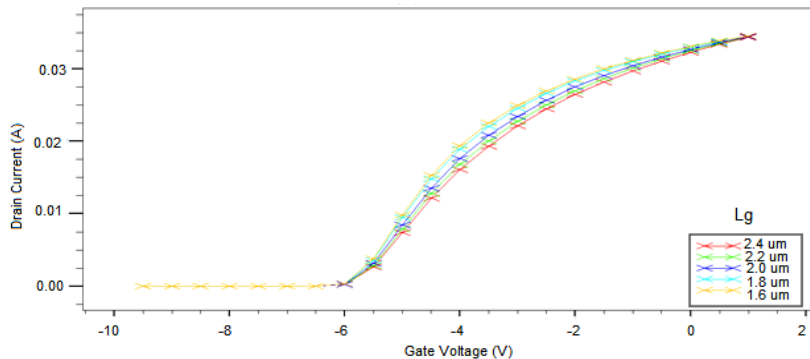
Fig. 3. *I-V* characteristics for I_d-V_{gs} at varying (L_g).
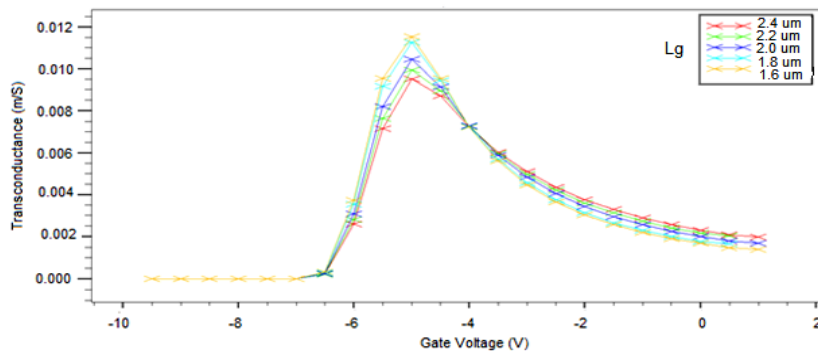
Fig. 4. g_m against voltage gate at varying (L_g).
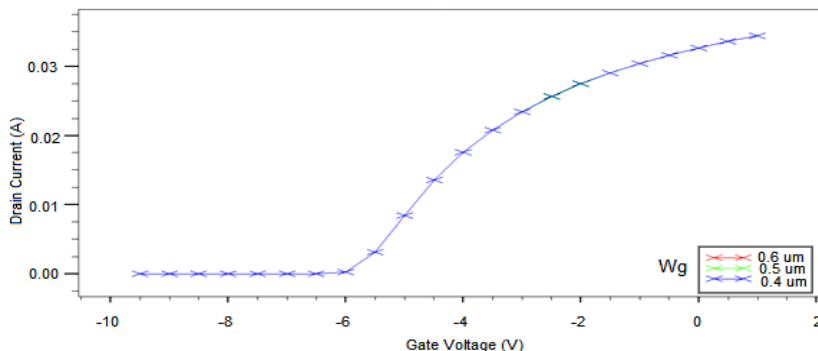
Fig. 5. *I-V* characteristics for I_d-V_{gs} at varying (W_{ch}).
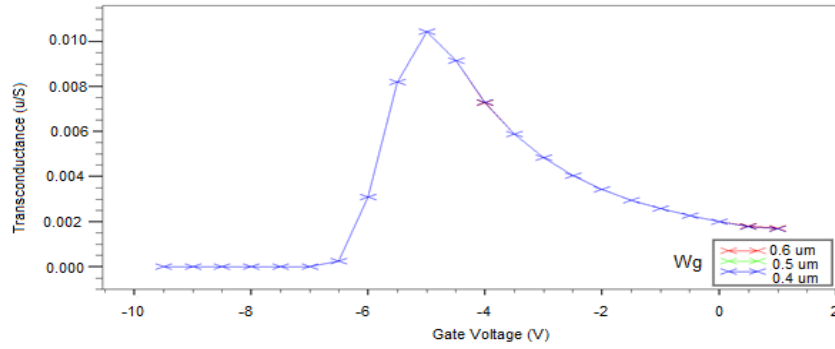
Fig. 6. g_m against voltage gate at varying (W_{ch}).
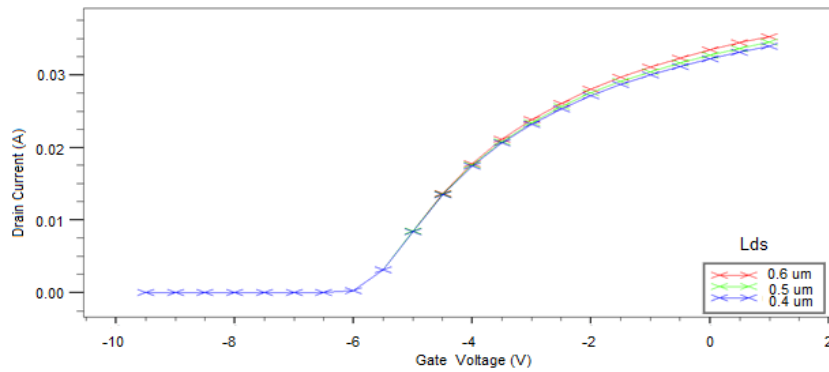
Fig. 7. *I-V* characteristics for I_d-V_{gs} at varying (L_{sd}).
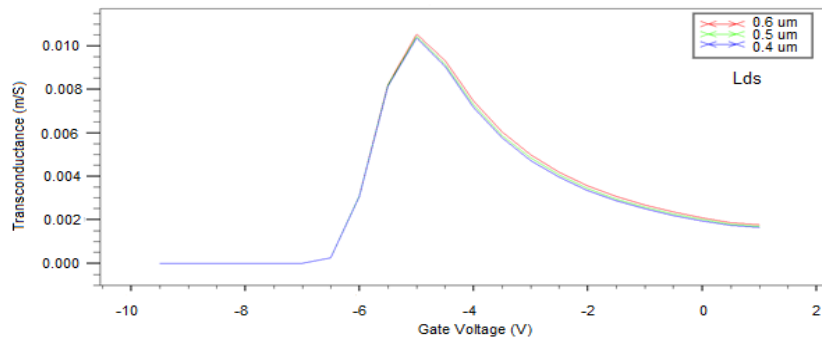
Fig. 8. g_m versus voltage gate at varying (L_{sd}).

Fig. 6 shows the transconductance (g_m) against gate voltage (V_g) at different values of (W_{ch}). We noticed that when the channel width decreases the transconductance is increased. Wherein the g_m is 28.80 m/s at a channel width is 0.5 µm and the g_m is 28.98 m/s at a channel width is 1.6 µm.

Fig. 6 demonstrates the device's effectiveness by showing that g_m will increase when W_{ch} decreases. That implies that the ratio between them (g_m and W_{ch}) is reversed. Reducing the length to width ratio of the channel may shows an effects on the current flow as the gate control for the current becomes limited. But the punch-through of current may accours.

C. Downscaling Length of Source and Drain

Fig. 7 depicts the transfer characteristics of the drain current (I_d) with the gate voltage (V_g) at the different values of (Lds). We noticed that the relationship between (I_d and V_{gs}) is a direct relationship, where the length of (source and drain) increased hence drain current is increased. Drain current is equal to 33.91 mA at a length of 0.4 µm and the drain current is equal to 35.29 mA at 0.6 µm for the length of (source and drain) respectively.

While threshold voltage (V_t) is reverse proportional to length (L_{ds}), where V_t is equal to −12.52V at L_{ds} = 0.4 µm and V_t is equal to −11.74 V at L_{ds} = 0.6 µm. The figure clear up the performance of the device when L_{ds} will increase the V_t decreases. That implies that the ratio between (L_{ds} and V_t) is reversed.

Fig. 8 illustrates the transconductance (g_m) against gate voltage (V_g) at different values of (L_{ds}). We noticed that when the length of the (source and drain) is increased the transconductance is increased. Wherein the gm is 28.50 m/s at L_{ds} = 0.4 µm and L_{ds} is 28.93 m/s at L_{ds} = 0.6 µm.

D. Downscaling Width of the Material (GaN)

Fig. 9 shows the transconductance (g_m) against the different values of the width material of GaN. We noticed that when the width of the material increases the transconductance is increased. Wherein the gm is 17.56 m/s at GaN = 1.5 µm and gm is 28.80 m/s at GaN = is 2.0 µm. The last figure boost the capability of the device, wherein when the width of the GaN increased the gm increased also. That reveals that the ratio between them is direct.
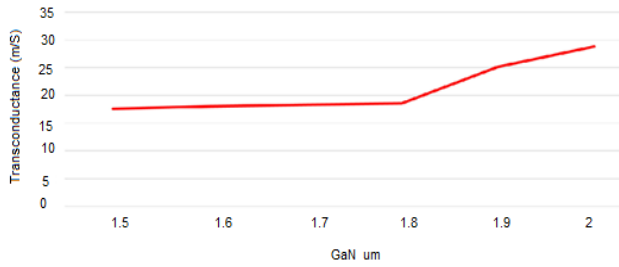
Fig. 9. g_m versus width of GaN.

V. RESULTS COMPARISON

When compared between the obtained results from this work with other related works, we notice that some of the performances of electrical characteristics are improved as compared to the previous works as shown in Table I. The operating conditions of all parameters are done at temperature=300K. The transconductance g_m was 13 m/s, 17 m/s, 19 m/s and 2 m/s, respectively reported in [45−47], while according to our results, we obtained g_m = 27.87 m/s, 28.80 m/s, 29.02 m/s and 29.91 m/s, respectively. As we know, the higher of the trans-conductance value, that's mean the better and improved performance. The reason for increased in ($g_m =\partial I_d/\partial V_g$) is direct proportional with the saturation of drain current. I_{ON}/I_{OFF} ratio was 6×10^8, 2.3×10^8, 2.1×10^9 and 1×10^{10}, respectively reported in [48−51] while we obtained I_{ON}/I_{OFF} = 19.65×10^{14}, 26.91×10^{15}, 28.23×10^{15} and 34.44×10^{15}, respectively. The higher of I_{ON}/I_{OFF} ratio, that's mean the better and improved performance. The reason for increased in I_{ON}/I_{OFF} ratio is high electron mobility obtained of channel along with the reduction in source/drain parasitic resistance. Finally the threshold voltage V_t was 4.2, 5.0, 6.28 and 7.6V, respectively reported in [51−54], while we obtained V_t =−10.29 V, −11.43 V, −11.92 V and −12.09V, respectively. Subthreshold slop SS (mv/dec) has not seen significant improvement.

The difference between this work and others related works is the result of different working conditions, type of material layer used in fabricated channel, type of deposition layers, temperature circumstances, engineering method for device manufactured, type of dielectric constant and device dimensions.

TABLE I: PERFORMANCE COMPARISON OF WITH RELATED WORKS

V_t (V) *	V_t (V)	Operating conditions	I_{ON}/I_{OFF} *	I_{ON}/I_{OFF}	Operating conditions	g_m (m/S) *	g_m (m/S)	Operating conditions
−10.29	4.2 [51]	TiO$_2$(3.4 nm)	19.65×10^{14}	6×10^8 [49]	VGS = 12 V	27.87	13 [46]	R$_{ON}$ = 12 Ω. mm
−11.43	5.0 [54]	Al$_2$O$_3$ (20 nm)	26.91×10^{15}	2.3×10^8 [51]	VGS = 15 V	28.80	17 [47]	R$_{ON}$ = 13.2 Ω. mm
−11.92	6.28 [52]	SiN (30 nm)	28.23×10^{15}	2.1×10^9 [50]	VGS = 6.5 V	29.02	19 [45]	R$_{ON}$ = 7.4 Ω. mm
−12.09	7.6 [53]	Al$_2$O$_3$ (18 nm)	34.44×10^{15}	1.0×10^{10} [48]	VGS = 6 V	29.91	2 [46]	R$_{ON}$ = 26 Ω. mm

* This work

VI. CONCLUSION

This article examined and evaluated the impact of changing the dimensions of the HEMT device based on channel length (L_g), the width of the channel (W_{ch}), length of the source and drain (L_{ds}) and width of the material (GaN) on the electrical characteristics of the device such as I_{ON}, I_{ON}/I_{OFF}, and gm. By Technology Computer-Aided Design (TCAD) tool, we could build a new structure and gain improved specifications to enhance the performance of the device. Optimal results were obtained at channel length L_g = 1.6 µm, where I_{ON} = 34.56 mA, I_{ON}/I_{OFF} = 19.63×10^{15} and g_m = 29.91 m/s. According to the width of the channel, the optimal results at W_{ch} = 0.3µm, where I_{ON} = 34.48 mA, I_{ON}/I_{OFF} = 24.80×10^{15} and g_m = 28.98 m/s, while the length of source and drain L_{ds} = 0.6 µm, I_{ON} = 35.29 mA, I_{ON}/I_{OFF} = 28.23×10^{15} and g_m = 28.93 m/s. Finally, the width of the material at GaN = 2 µm, I_{ON} = 34.48 mA, I_{ON}/I_{OFF} = 26.12×10^{15} and g_m = 28.80 m/s.

CONFLICT OF INTEREST

The authors declare no conflict of interest.

AUTHOR CONTRIBUTIONS

Firas Natheer Abdul-kadir: formulating the idea, designing the experiments, presenting the results; Nawfel Y. Jamil: literature review, performing the experiments, collecting and presenting the results; Laith Al Taan: writing and editing the paper; Waheb A. Jabbar: revising and formatting the final version.

ACKNOWLEDGMENT

REFERENCES

[1] H. Rodilla, B. G. Vasallo, J. Mateos, G. Moschetti, J. Grahn, and T. González, "Monte carlo study of the noise performance of isolated-gate InAs HEMTs," in *Proc. of 2011 21st International Conference on Noise and Fluctuations*, Toronto, Canada, 2011, pp. 184-187.

[2] S. Ganguly, J. Verma, Z. Hu, H. (Grace) Xing, and D. Jena, "Performance enhancement of InAlN/GaN HEMTs by KOH surface treatment," *Appl. Phys. Express*, vol. 7, no. 3, #034102, 2014.

[3] M. S. Begum, J. Vijayashree, A. Mohanbabu, and N. Mohankumar, "Investigation of performance of InAsSb based high electron mobility transistors (HEMTs)," in *Proc. of 2017 Devices for Integrated Circuit (DevIC)*, Kalyani, India, 2017, pp. 699-701.

[4] P. Pal, Y. Pratap, M. Gupta, S. Kabra, and H. D. Sehgal, "Performance analysis of ScAlN/GaN high electron mobility transistor (HEMT) for biosensing application," in *Proc. of 2020 5th International Conference on Devices, Circuits and Systems (ICDCS)*, Coimbatore, India, 2020, pp. 203-206.

[5] D. McMorrow, J. B. Boos, D. Park, S. Buchner, A. R. Knudson, and J. S. Melinger, "Charge-collection dynamics of InP-based high electron mobility transistors (HEMTs)," *IEEE Trans. on Nuclear Science*, vol. 49, no. 3, pp. 1396-1400, June 2002.

[6] Q. Meng Q. Lin F. Han W. Jing Y. Wang, and Z. Jiang, "A terahertz detector based on double-channel GaN/AlGaN high electronic mobility transistor," *Materials (Basel)*, vol. 14, no. 20, Oct. 2021, doi: 10.3390/ma14206193

[7] O. Zeggai, A. Ould-Abbas, M. Bouchaaour, *et al.*, "Biological detection by high electron mobility transistor (HEMT) based AlGaN/GaN," *Physica Status Solidi*, vol. 11, no. 2, pp. 274-279, 2014.

[8] S. Anwar, S. M. Gulfam, B. Muhammad, *et al.*, "Analysis and characterization of normally-off gallium nitride high electron mobility transistors," *Computers, Materials & Continua*, vol. 69, no. 1, pp. 1021–1037, 2021.

[9] A. Amar, B. Radi, and A. El Hami, "Electrothermal reliability of the high electron mobility transistor (HEMT)," *Appl. Sci.*, vol. 11, no. 22, #10720, 2021, https://doi.org/10.3390/app112210720

[10] V. Hemaja and D. K. Panda, "A comprehensive review on high electron mobility transistor (HEMT) based biosensors: Recent advances and future prospects and its comparison with Si-based biosensor," *Silicon*, vol. 14, pp. 1873–1886, 2022, https://doi.org/10.1007/s12633-020-00937-w

[11] F. N. Abdul-kadir, Y. Hashim, M. N. Shakib, and F. H. Taha, "Electrical characterization of Si nanowire GAA-TFET based on dimensions downscaling," *International Journal of Electrical and Computer Engineering (IJECE)*, vol. 11, no. 1, pp. 780-787, 2021.

[12] M. N. A. Aadit, S. G. Kirtania, F. Afrin, *et al.*, "High electron mobility transistors: performance analysis, research trend and applications," in *Different Types of Field-Effect Transistors - Theory and Applications*, M. M. Pejovic and M. M. Pejovic, Ed. 2017, http://dx.doi.org/10.5772/67796

[13] W. Xing, Z. Liu, G. I. Ng, and T. Palacios, "Temperature dependent characteristics of InAlN/GaN HEMTs for mm-Wave Applications," *Procedia Engineering*, vol. 141, pp. 103-107, 2016.

[14] M. A. Alim, C. Gaquiere, and G. Crupi, "An experimental and systematic insight into the temperature sensitivity for a 0.15-µm gate-length HEMT based on the GaN technology," *Micromachines*, vol. 12, no. 5, 2021, https://doi.org/10.3390/mi12050549

[15] Z. Guo and T. P. Chow, "Performance evaluation of channel length downscaling of various high voltage AlGaN/GaN power HEMTs," *Physica Status Solidi*, vol. 212, no. 5, pp. 1137-1144, 2015.

[16] N. Islam, M. F. P. Mohamed, M. F. A. J. Khan, *et al.*, "Reliability, applications and challenges of GaN HEMT technology for modern power devices: A review," *Crystals*, vol. 12, no. 11, 2022, https://doi.org/ 10.3390/cryst12111581

[17] W. A. Jabbar, A. Mahmood, and J. Sultan, "Modeling and characterization of optimal nano-scale channel dimensions for fin field effect transistor based on constituent semiconductor materials," *TELKOMNIKA Telecommunication Computing Electronics and Control*, vol. 20, no. 1, pp. 221-234, 2022.

[18] F. N. Abdul-kadir and F. H. Taha, "Characterization of silicon tunnel field effect transistor based on charge plasma," Indonesian *Journal of Electrical Engineering and Computer Science*, vol. 25, no. 1, pp. 138-143, 2022.

[19] S. Lee, M. Hashisaka, T. Akiho, *et al.*, "Cryogenic GaAs high-electron-mobility-transistor amplifier for current noise measurements," *The Review of Scientific Instruments*, vol. 92, 2021, https://doi.org/10.1063/5.0036419

[20] Y. C. Lin, S. H. Chen, P. H. Lee, *et al.*, "Gallium nitride (GaN) high-electron-mobility transistors with thick copper metallization featuring a power density of 8.2 W/mm for Ka-band applications," *Micromachines*, vol. 11, no. 2, 2020, doi:10.3390/mi11020222

[21] K. H. Hamza, D. Nirmal, A. S. A. Fletcher, *et al.* "Highly scaled graded channel GaN HEMT with peak drain current of 2.48 A/mm," *AEU-International Journal of Electronics and Communications*, vol. 136, #153774, Jul. 2021.

[22] F. N. AbdulKadir, K. K. Mohammad, and Y. Hashim, "Investigation and design of ion implanted MOSFET based on (18 nm) channel length," *Telkomnika (Telecommunication Comput. Electron. Control)*, vol. 18, no. 5, pp. 2635–2641, 2020.

[23] M P. Sruthi, A. Shanbhag, A. Chakravorty, N. DasGupta, and A. DasGupta, "Physics based Compact Model for Drain Current in Fin-Shaped GaN MIS-HEMTs," in *Proc. of 2021 IEEE BiCMOS and Compound Semiconductor Integrated Circuits and Technology Symposium (BCICTS)*, Monterey, CA, USA, 2021, doi: 10.1109/BCICTS50416.2021.9682482

[24] A. Amar, B. Radi, and A. El Hami, "Optimization based on electro-thermo-mechanical modeling of the high electron mobility transistor (HEMT)," *International Journal for Simulation and Multidisciplinary Design Optimization*, vol. 13, 2022, doi:10.1051/smdo/2021035

[25] J. Singh, A. Verma, V. K. Tewari, *et al.*, "Design and parametric analysis of GaN on silicon high electron mobility transistor for RF performance enhancement," *Silicon*, vol. 14, pp. 6311–6319, 2022, https://doi.org/10.1007/s12633-021-01419-3

[26] S. S. Mahajan, A. Malik, R. Laishram, *et al.*, "Performance enhancement of gate-annealed AlGaN/GaN HEMTs," *Journal of the Korean Physical Society*, vol. 70, pp. 533–538, 2017, https://doi.org/10.3938/jkps.70.533

[27] A. Amar, B. Radi, and A. El Hami, "Reliability based design optimization applied to the high electron mobility transistor (HEMT)," *Microelectronics Reliability*, vol. 124, #114299, 2021.

[28] A. M. Bhat, N. Shafi, R. Poonia, *et al.*, "Design and analysis of a field plate engineered high electron mobility transistor for enhanced performance," *J. Electron. Mater.*, vol. 51, pp. 3773–3781, 2022, https://doi.org/10.1007/s11664-022-09646-z

[29] E. E. Patrick, M. Choudhury, F. Ren, *et al.*, "Simulation of Radiation Effects in AlGaN/GaN HEMTs," *ECS Journal of Solid State Science and Technology*, vol. 4, no. 3, doi: 10.1149/2.0181503jss

[30] Y. Liu, T. Egawa, and H. Jiang, "Enhancement-mode quaternary AlInGaN/GaN HEMT with non-recessed-gate on sapphire substrate," *Electron. Lett.*, vol. 42, no. 15, pp. 884-886, 2006.

[31] T. Tamura, J. Kotani, S. Kasai, and T. Hashizume, "Nearly temperature-independent saturation drain current in a multi-mesa-channel AlGaN/GaN high electron mobility transistor," *Appl. Phys. Exp.*, vol. 1, no. 2, #023011, Feb. 2008.

[32] S. Takashima, Z. Li, and T. P. Chow, "Sidewall dominated characteristics of fin-gate AlGaN/GaN MOS-channel-HEMTs," *IEEE Trans. Electron Devices*, vol. 60, no. 10, pp. 3025-3031, Oct. 2013.

[33] M. A. Alsharef, R. Granzner, and F. Schwierz, "Theoretical investigation of trigate AlGaN/GaN HEMTs," *IEEE Trans. Electron Devices*, vol. 60, no. 10, pp. 3335-3341, Oct. 2013.

[34] M. Haziq, S. Falina, A. Manaf, *et al.*, "Challenges and opportunities for high-power and high-frequency AlGaN/GaN high-electron-mobility transistor (HEMT) applications: A Review," *Micromachines*, vol. 13, no. 12, 2022, https://doi.org/10.3390/mi13122133

[35] L. Geng, H. Zhao, T. Han, and X. Ren, "The lattice-matched AlInN/GaN high electron mobility transistor with BGaN buffer," *Solid State Communications*, vol. 337, #114449, Oct. 2021, doi: 10.1016/j.ssc.2021.114449

[36] F. Heinz, F. Thome, A. Leuther, and O. Ambacher, "A 50-nm gate-length metamorphic HEMT technology optimized for cryogenic ultra-low-noise operation," *IEEE Trans. on Microwave Theory and Techniques*, vol. 69, no. 8, pp. 3896-3907, Aug. 2021.

[37] J. He, W. C. Cheng, Q. Wang, *et al.*, "Recent advances in GaN-based power HEMT devices," *Advanced Electronic Materials*, vol. 7, no. 4, #2001045, April 2021.

[38] G. Greco, F. Iucolano, and F. Roccaforte, "Review of technology for normally-off HEMTs with p-GaN gate," *Materials Science in Semiconductor Processing*, vol. 78, pp. 96-106, 2018.

[39] W. Zhang, X. Huang, Z. Liu, *et al.*, "A new package of high-voltage cascode gallium nitride device for megahertz operation," *IEEE Trans. on Power Electronics*, vol. 31, no. 2, pp. 1344-1353, 2015.

[40] J. Ajayan, D. Nirmal, P. Mohankumar, *et al.*, "Challenges in material processing and reliability issues in AlGaN/GaN HEMTs on silicon wafers for future RF power electronics & switching applications: A critical review," *Materials Science in Semiconductor Processing*, vol. 151, #106982, Nov. 2022.

[41] H. Hamada, T. Fujimura, I. Abdo, *et al.*, "300-GHz. 100-Gb/s InP-HEMT wireless transceiver using a 300-GHz fundamental mixer," in *Proc. of IEEE/MTT-S International Microwave Symposium*, 2018, pp. 1480-1483.

[42] S. Khandelwal, N. Goyal, and T. A. Fjeldly, "A physics-based analytical model for 2DEG charge density in AlGaN/GaN HEMT devices," *IEEE Trans. Electron Devices*, vol. 58, no. 10, pp. 3622-3625, Oct. 2011.

[43] Z. Huang, W. Yan, Z. Li, H. Dong, and F. Yang, "Modelling effects of GaN HEMTs terahertz detectors with spiral antennas," *Proc. of SPIE*, vol. 12061, pp. 92-96, 2021.

[44] S. C. Kang, H. W. Jung, S. J. Chang, *et al.*, "Charging effect by fluorine-treatment and recess gate for enhancement-mode on

algan/gan high electron mobility transistors," *Nanomaterials*, vol. 10, no. 11, #2116, 2020.

[45] H. Xue, K. Hussain, V. Talesara, *et al*., "High-Current-Density enhancement-mode ultrawide-bandgap AlGaN channel metal-insulator-semiconductor heterojunction field-effect transistors with a threshold voltage of 5 V," Physica Status Solidi (RRL)-Rapid Research Letters, vol. 15, no. 6, p. 2000576, 2021.

[46] X. Cai, M. Hua, Z. Zhang, *et al*., "Atomic-scale identification of crystalline GaON nanophase for enhanced GaN MIS-FET channel," *Applied Physics Letters*, vol. 114, no. 5, #053109, Feb. 2019.

[47] M. Hua, J. Wei, J. Lei, *et al*., "Integration of LPCVD-SiNx gate dielectric with recessed-gate E-mode GaN MIS-FETs: Toward high performance, high stability and long TDDB lifetime," in *Proc. of 2016 IEEE International Electron Devices Meeting*, San Francisco, USA, 2016, doi: 10.1109/IEDM.2016.7838388.

[48] L. Nela, M. Zhu, J. Ma, and E. Matioli, "High-performance nanowire-based E-mode power GaN MOSHEMTs with large work-function gate metal," *IEEE Electron Device Letters*, vol. 40, no. 3, pp. 439–442, 2019.

[49] M. Li, J. Wang, B. Zhang, *et al.*, "Improved fabrication of fully-recessed normally-off SiN/SiO$_2$/GaN MISFET based on the self-terminated gate recess etching technique," *Solid-State Electronics*, vol. 177, p. 107927, 2021.

[50] F. Azam, A. Tanneeru, B. Lee, and V. Misra, "Engineering a unified dielectric solution for AlGaN/GaN MOS-HFET gate and access regions," *IEEE Transactions on Electron Devices*, vol. 67, no. 3, pp. 881–887, 2020.

[51] A. Rawat, A. Meer, M. Surana, *et al.*, "Thermally grown TiO$_2$ and Al$_2$O$_3$ for GaN-based MOS-HEMTs," *IEEE Transactions on Electron Devices*, vol. 65, no. 9, pp. 3725–3731, 2018.

[52] B. Zhang, J. Wang, C. Huang, *et al*., "Improved performance of fully-recessed high-threshold-voltage GaN MIS-HEMT with in situ H2/N2 plasma pretreatment," *IEEE Electron Device Letters*, vol. 43, no. 7, pp. 1021-1024, 2022.

[53] Q. Zhou, A. Zhang, B. Chen, *et al*., "7.6 V threshold voltage high-performance normally-off Al$_2$O$_3$/GaN MOSFET achieved by interface charge engineering," *IEEE Electron Device Letters*, vol. 37, no. 2, pp. 165-168, 2016.

[54] J. T. Asubar, S. Kawabata, H. Tokuda, A. Yamamoto, and M. Kuzuhara, "Enhancement-mode AlGaN/GaN MIS-HEMTs with high V TH and high I Dmax using recessed-structure with regrown AlGaN barrier," *IEEE Electron Device Letters*, vol. 41, no. 5, pp. 693–696, 2020.

Firas N. Abdul-kadir received the B.Sc. degree in medical instruments engineering from Mosul Technical College and Master degree of engineering in electronics and communications engineering from the University of Mosul, Mosul, Iraq, in 1998 and 2013 respectively. He is currently an Assistant Lecturer in the Department of Electrical Engineering, College of Engineering, Mosul University, Mosul, Iraq. His research interests include Microelectronics and Nano electronic, MOSFET nono-structure.

Nawfal Y. Jamil received a B.Sc. in Physics from Mosul University, a Master of thin film from Mosul University, and a Ph.D. in Solid State from Hull University, England, in 1980 and 1990 respectively. Currently, he is a Assistant Professor and a Head of the department at Al-Noor University College, IRAQ. His research interests include semiconductor devices and thin-film tech.

Laith M. Altaan received a B.Sc. in Physics from Mosul University, a Master of Microwave from Basrah University, and a Ph.D. in Solid State Electronics from the University of Mosul, Mosul, Iraq, in 1990 and 2004 respectively. He is currently a Professor in the Department of Physics, College of Science, Mosul University, Iraq. His research interests include semiconductor devices, microwave antennas, and thin films.

Waheb A. Jabbar received the B.Sc. in Electrical Engineering from the University of Basrah, Iraq, in 2001, the M.Eng. in Communication & Computer and the Ph.D. in Electrical, Electronics, and System Engineering from Universiti Kebangsaan Malaysia (UKM), Bangi, Selangor, Malaysia, in 2011 and 2015 respectively. He is currently an Associate Professor at Birmingham City University, Birmingham, United Kingdom. His research interests include Mobile Communications, Wireless Networking, Advanced Electronics and Automation. He also has a keen interest in Internet of Things and Smart City.